Chemistry & Biology
Article

Cell PRESS

Droplet-Based Microfluidic Platforms for the Encapsulation and Screening of Mammalian Cells and Multicellular Organisms

Jenifer Clausell-Tormos,[1,2,4] Diana Lieber,[1,2,4] Jean-Christophe Baret,[1,2] Abdeslam El-Harrak,[1,2] Oliver J. Miller,[1,2] Lucas Frenz,[1,2] Joshua Blouwolff,[1,2,3] Katherine J. Humphry,[3] Sarah Köster,[3] Honey Duan,[3] Christian Holtze,[3] David A. Weitz,[3] Andrew D. Griffiths,[1,2,*] and Christoph A. Merten[1,2,*]
[1]Institut de Science et d'Ingénierie Supramoléculaires, Université Louis Pasteur
[2]CNRS UMR 7006
8 allée Gaspard Monge, 67083 Strasbourg Cedex, France
[3]School of Engineering and Applied Sciences/Department of Physics, Harvard University, Cambridge, MA 02138, USA
[4]These authors contributed equally to this work.
*Correspondence: cmerten@isis.u-strasbg.fr (C.A.M.), griffiths@isis.u-strasbg.fr (A.D.G.)
DOI 10.1016/j.chembiol.2008.04.004

SUMMARY

High-throughput, cell-based assays require small sample volumes to reduce assay costs and to allow for rapid sample manipulation. However, further miniaturization of conventional microtiter plate technology is problematic due to evaporation and capillary action. To overcome these limitations, we describe droplet-based microfluidic platforms in which cells are grown in aqueous microcompartments separated by an inert perfluorocarbon carrier oil. Synthesis of biocompatible surfactants and identification of gas-permeable storage systems allowed human cells, and even a multicellular organism (*C. elegans*), to survive and proliferate within the microcompartments for several days. Microcompartments containing single cells could be reinjected into a microfluidic device after incubation to measure expression of a reporter gene. This should open the way for high-throughput, cell-based screening that can use >1000-fold smaller assay volumes and has ~500× higher throughput than conventional microtiter plate assays.

INTRODUCTION

Miniaturization has been the feature that has enabled many of the most dramatic technological developments in recent decades. In electronics, the number of transistors per integrated circuit has roughly doubled every 2 yr since their invention in 1961. Miniaturization in biology and chemistry, although important, has been much less dramatic. Reaction volumes have typically been reduced from a few milliliters (in test tubes) to a few microliters (in microtiter plates)—a reduction of only 1000-fold. Nevertheless, today, high-throughput screening (HTS) programs can process up to 100,000 compounds per d (~1 s^{-1}). Unfortunately, there is little scope for further miniaturization of microtiter-plate technology due to evaporation and capillary action causing "wicking" and bridging of liquid between wells (Dove, 1999).

A promising approach to overcome these limitations is to use microfluidic systems, which consist of networks of channels of typically 10–100 μm diameter. Small quantities of reagents can be brought together in a specific sequence, mixed, and allowed to react for a specified time in a controlled region of the channel network by using electrokinetic and/or hydrodynamic pumping (Li and Harrison, 1997; Lin et al., 2001). They are being developed for use in several areas, allowing, for example, protein purification, DNA separation, and PCR on a drastically decreased scale (Hawtin et al., 2005; Wang, 2002). The ability to rapidly fabricate microfluidic devices in poly(dimethylsiloxane) (PDMS) by using soft lithography (Squires and Quake, 2005) has greatly stimulated the development of microfluidic systems. It has even enabled sophisticated microfluidic arrays containing thousands of compartments separated by valves (Thorsen et al., 2002).

Even though commercial microfluidic lab-on-a-chip systems already represent a serious competing technology for 1536-well plates for certain types of screen, the laminar flow in microfluidic devices creates two problems (Song et al., 2003). First, mixing is slow; second, the concentration of reagents changes continuously in the microchannels due to diffusion and the parabolic flow profile. Additionally, crosscontamination can create serious problems. These problems can be overcome by using systems in which the individual assays are compartmentalized in aqueous microdroplets, separated by immiscible oil. Non-microfluidic systems based on the compartmentalization of reactions in aqueous microdroplets of water-in-oil (w/o) emulsions were originally developed for directed evolution and have since been applied in a number of areas (Tawfik and Griffiths, 1998; Kelly et al., 2007; Griffiths and Tawfik, 2006), including ultra-high-throughput sequencing (Margulies et al., 2005; Shendure et al., 2005). However, making and manipulating droplets in two-phase (droplet-based) microfluidic systems allows for a level of control of picoliter scale biochemical assays that was hitherto impossible. Highly monodisperse (<3% polydispersity) w/o drops can be generated at frequencies greater than 10 kHz (Umbanhowar et al., 2000; Thorsen et al., 2001; Anna et al., 2003). Furthermore, the aqueous microdroplets can be fused or subdivided (Link et al., 2004, 2006; Ahn et al., 2006), the contents of microdroplets can be mixed rapidly, and sorting

modules allow for the specific enrichment of microdroplets (Song et al., 2003; Link et al., 2006; Ahn et al., 2006). Droplet-based microfluidic systems based on the formation of arrays of plugs (droplets that fill the microfluidic channels) have also been developed (Chen and Ismagilov, 2006). Each aqueous sample plug is stored in a holding component (e.g., a piece of tubing or a capillary) and is spaced by a second immiscible liquid or gas. In this way, microcompartments can be generated and stably separated without the use of any surfactant.

Droplet-based microfluidic systems have been used for a range of different applications, including single-molecule PCR, proteome analysis, clinical diagnosis on human physiological fluids, protein crystallization, and titration of anticoagulants (Beer et al., 2007; Wheeler et al., 2005; Srinivasan et al., 2004; Chen and Ismagilov, 2006; Song et al., 2006). They have also been used to encapsulate prokaryotic and eukaryotic cells (Martin et al., 2003; Grodrian et al., 2004; Sakai et al., 2005; He et al., 2005; Oh et al., 2006; Huebner et al., 2007), and even the embryos of multicellular organisms (Funfak et al., 2007). However, neither the incubation and/or recovery of viable mammalian cells nor a full life cycle of an encapsulated multicellular organism was demonstrated. Furthermore, none of those systems allowed for an automated analysis of individual compartments subsequent to an incubation period as required for high-throughput, cell-based assays.

We present here two complementary droplet-based microfluidic platforms that allow fully viable human cells to be recovered with high yield after several days in microcompartments. The volume of each microcompartment can be over 1,000-fold smaller than the smallest volumes utilizable in microtiter-plate-based assays, and single or multiple human cells, as well as multicellular organisms such as *C. elegans*, can be compartmentalized and can replicate in these systems. To prove the utility of this approach for cell-based assays, we also demonstrate automated fluorescence-based analysis of single cells in individual compartments after 16 hr of incubation.

RESULTS

Emulsion-Based Encapsulation

The ultimate goal of this study was to set up microfluidic platforms for high-throughput, cell-based assays. Hence, the technology should allow for (1) Encapsulation of a predefined number of cells per microcompartment (with the option of encapsulating single cells being highly desirable), (2) storage of the compartmentalized samples within a CO_2 incubator, and (3) recovery of the cells from the compartments in a way that does not abolish cell viability.

The encapsulation step (Figures 1A and 1B; Movie S1, see the Supplemental Data available with this article online) was performed on a PDMS chip in which 660 pl drops (corresponding to a spherical diameter of 100 μm ± 1.7%) were created from a continuous aqueous phase by "flow focusing" with a perfluorinated carrier oil (Anna et al., 2003). Perfluorocarbon oils are perfectly suited for this purpose, since they are compatible with PDMS devices, immiscible with water, transparent (allowing for optical readout procedures), and have been shown to facilitate respiratory gas delivery to both prokaryotic and eukaryotic cells in culture (Lowe et al., 1998). The number of cells per
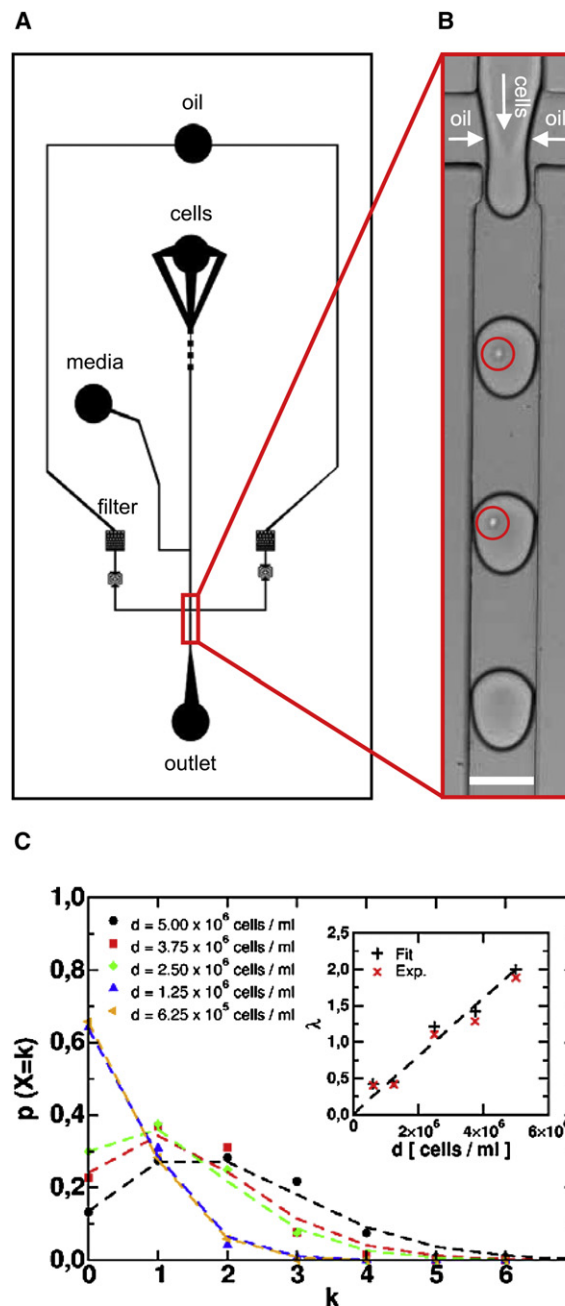

Figure 1. Encapsulation of Jurkat Cells into Aqueous Microdrops of a Water-in-Oil Emulsion

(A) Design of the microfluidic chip (main channels were 75 μm deep and 100 μm wide). The red rectangle indicates the section shown in (B), in which the drops are generated by flow focusing.

(B) Encapsulation of single Jurkat cells (highlighted by red circles) into 660 pl droplets at a frequency of 800 Hz. White bar, 100 μm.

(C) On-chip dilution of the cell-suspension allows for the controlled encapsulation of single cells (here: Jurkat cells). The experimentally determined probability (p, y axis) for the number of cells per drop (k, x axis) is in good agreement with a Poisson distribution (dashed lines) for various cell densities (resulting from on-chip dilution). Inset: the average number of cells per drop (λ) plotted against the cell density for the experimental data (Exp.) and the Poisson distribution (Fit). The dashed line is the theoretical number of cells per drop according to the cell density only (homogeneously distributed).

droplet was controlled by using on-chip dilution of the cells to regulate the cell density (Figure 1C): a culture of Jurkat cells, with an initial density of 5×10^6 cells/ml, was brought together with a stream of sterile medium by co-flow immediately before drop formation, and the relative flow rates of the cell suspension and the medium were changed, whereas the sum of the two flow rates was kept constant. The number of cells per drop (k) was always in good agreement with a Poisson distribution, and high cell densities at the nozzle ($\geq 2.5 \times 10^6$ cells/ml) made the encapsulation of multiple cells per drop highly likely (p > 30%). In contrast, cell densities of 1.25×10^6 cells/ml and below resulted in low probabilities (p $\leq$ 7%) for the encapsulation of more than one cell per drop (while increasing the probability of finding drops without any cells inside). At the same time, the average number of cells per drop (λ) decreased from approximately 2 (at 5×10^6 cells/ml) to far below 1 (at $\leq 1.25 \times 10^6$ cells/ml). Hence, the number of cells per drop can easily be regulated, even allowing for the compartmentalization of single cells.

The generation of stable drops requires the use of a surfactant that decreases the surface tension and, which for the encapsulation of cells, also has to be biocompatible. For this reason, we synthesized several perfluoropolyether-derived surfactants (PFPE surfactants) and tested their effect on long-term cell survival (Figure 2). The surfactants differed solely in their hydrophilic head groups, which should be the only part of the molecule in contact with the encapsulated cells. The common perfluorinated tail should be dissolved in the carrier oil and thus be oriented away from the cells. To analyze the biocompatibility, we seeded HEK293T cells on top of a perfluorocarbon oil layer in the presence (0.5% w/w) and absence of different surfactants. In the absence of any surfactant, the cells retained an intact morphology and even proliferated, whereas the ammonium salt of carboxy-PFPE (Johnston et al., 1996) and poly-L-lysine-PFPE (PLL-PFPE) mediated cell lysis. However, polyethyleneglycol-PFPE (PEG-PFPE) and dimorpholinophosphate-PFPE (DMP-PFPE) showed good biocompatibility, did not affect the integrity of the cellular membrane, and even allowed for cell proliferation. Since DMP-PFPE generated more stable emulsions than PEG-PFPE (data not shown), it was used for all further experiments.

As the next step, procedures allowing for the recovery of encapsulated cells had to be established. Addition of 15% (v/v) Emulsion Destabilizer A104 (RainDance Technologies) to the emulsions mediated reliable breaking without an obvious impact on cell viability. This allowed for the determination of the survival rates of suspension (Jurkat) and adherent (HEK293T) cells for different incubation times within drops. For this purpose, we encapsulated cells at a density corresponding to an average of less than 1 cell per 660 pl drop (1.25×10^6 cells/ml at the nozzle, resulting in a λ value of $\sim$0.55 and single cells in $\sim$31.7% of all drops) and collected the resulting emulsions in 15 ml centrifugation tubes. After different incubation times at 37°C within a CO_2 incubator, the emulsions were broken and the cells were treated with a live/dead stain to determine the survival rate and the total number (live and dead) of recovered cells (Figures 3A and 3C). During the first 4 d, the fraction of recovered viable Jurkat cells did not change significantly and was always in excess of 79%. Then, the percentage of live cells decreased from 71% after 5 d to 32% after 6 d and finally to 1% after 14 d of encapsulation. The total number of recovered cells divided by the number of
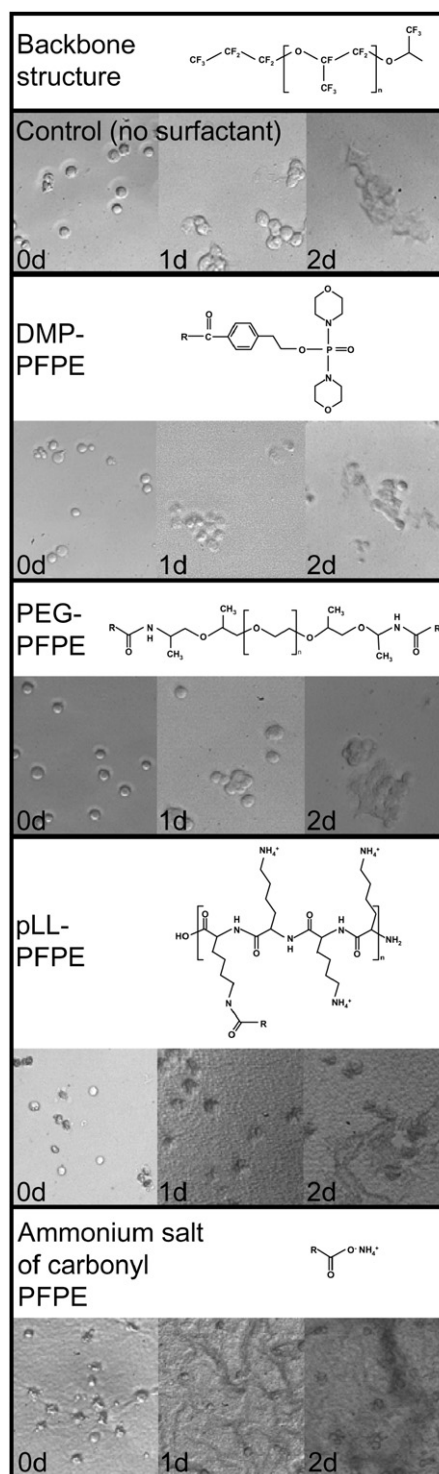

Figure 2. Surfactants Used to Generate the Emulsions
For each surfactant, the chemical structure and the results of the biocompatibility assay (microscopical bright-field images) are shown. For the assay, HEK293T cells were incubated for 48 hr on a layer of perfluorinated FC40 oil in the presence or absence (control) of the indicated surfactant (0.5% w/w).
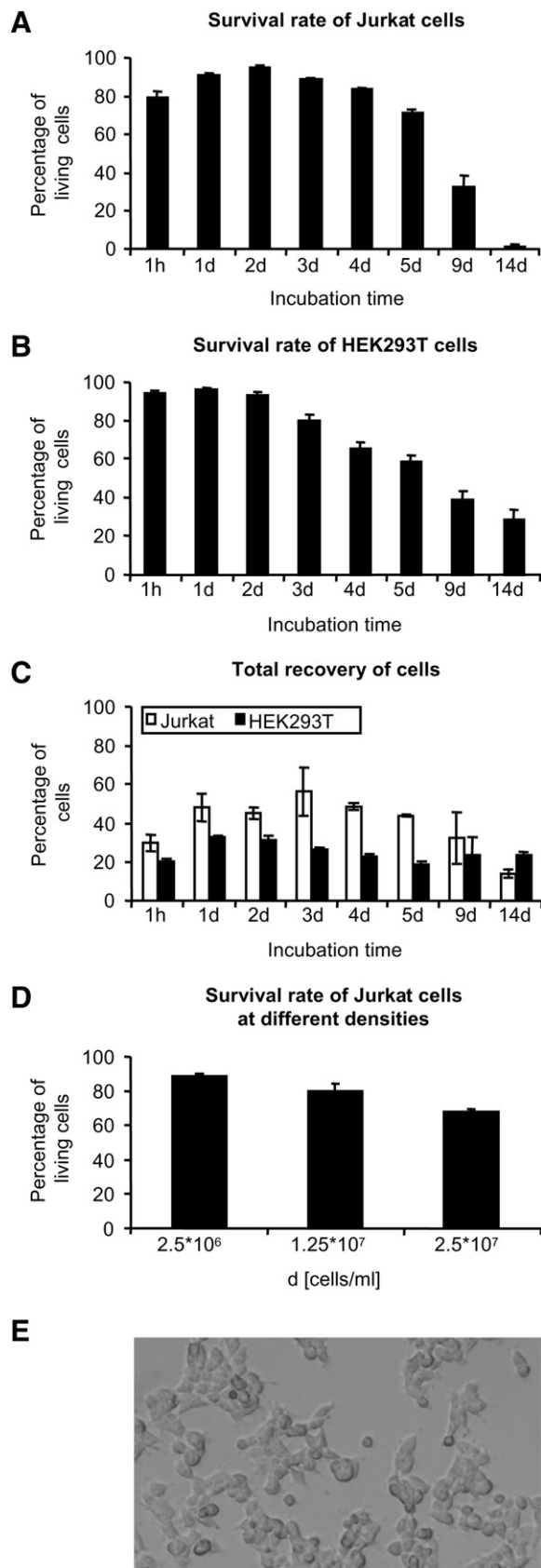
A Survival rate of Jurkat cells

B Survival rate of HEK293T cells

C Total recovery of cells

D Survival rate of Jurkat cells at different densities

E

Figure 3. Cell Viability, Recovery, and Recultivation of Cells Encapsulated in 660 pl Drops

(A and B) The percentage of viable (A) Jurkat and (B) HEK293T cells recovered from emulsions at the indicated time points.

(C) The total number of recovered Jurkat and HEK293T cells (live and dead) relative to the number of initially encapsulated cells.

(D) The percentage of viable Jurkat cells encapsulated at different densities after 3 d.

(E) Recultivation of HEK293T cells recovered after 48 hr of encapsulation.

Error bars show the standard deviation of three independent experiments.

initially encapsulated cells (equal to the aqueous flow rate multiplied by the injection time multiplied by the cell density at the nozzle) was defined as the recovery rate and increased from 29% after 1 hr to more than 55% after 2 d. This indicates some degree of proliferation within the drops, which is also supported by the fact that after 24 hr the percentage of dead cells was lower than after 1 hr. During further incubation within drops, the recovery rates slowly decreased to just 14% after 14 d. This decrease can be explained by the fact that dead cells ultimately disintegrate (after several days) and thus cannot be stained anymore. This effect is well known and has been analyzed in detail for bacterial cells (Villarino et al., 2000). However, early time points and the live stain are not affected by this phenomenon. When repeating the experiments with adherent HEK293T cells, similar results were obtained (Figures 3B and 3C). During the first 2 d, the fraction of recovered viable cells remained constant at more than 90% before slowly decreasing to 58% after 5 d and 39% after 9 d. Finally, after 14 d of encapsulation, 28% of the recovered cells were still alive. The total recovery rate increased slightly from 20% after 1 hr to more than 32% after 2 d. During further incubation within drops, the recovery rates slowly decreased to 23% after 14 d. The longer cell survival compared to Jurkat cells is most likely explained by slower proliferation, resulting in slower consumption of the available nutrition. Recovered cells could also be recultivated (instead of stained) after incubation for 2 d within droplets, resulting in normally proliferating cells (Figure 3E).

In an additional experiment, we assessed the effect of the cell density on the survival rates. For this purpose, we used 5- and 10-fold higher densities of Jurkat cells than used initially. Comparison of the cell survival after 3 d showed that the cell density inversely correlated with the survival rate (Figure 3D). Whereas almost 90% of viable cells were recovered by using the initial cell density, only 80% and 68%, respectively, survived for the 5- and 10-fold increased cell density. Insufficient gas exchange can be ruled out, since equally dense cultures in ordinary tissue-culture flasks did not survive longer: using a density equal to 1 cell in a 660 pl drop ($\sim 1.5 \times 10^6$ cells/ml), the number of viable Jurkat cells remained above 87% for the first 2 d, before decreasing to 51% after 4 d and 0% after 9 d (data not shown). Therefore, we conclude that the encapsulated cells most likely die due to the lack of nutrition or the accumulation of toxic metabolites, not because of compartmentalization-specific factors such as the oil and surfactant.

Plug-Based Encapsulation

In parallel to encapsulating cells into aqueous drops of a w/o emulsion, we established a system in which aqueous plugs spaced by immiscible oil within a piece of tubing serve as

a culture vessel. This approach allows for the generation of aqueous microcompartments big enough to host small cell populations and even multicellular organisms. This cannot be achieved by simply increasing the drop size of a given emulsion. First, the maximum size of a drop generated on a microfluidic chip is limited by the channel dimensions. Second, as the size of the drops increases, they become less stable, resulting in uncontrolled sample coalescence. These problems can be circumvented by alternately aspirating aqueous plugs and immiscible oil into a holding cartridge (e.g., a capillary or a piece of tubing) (Chen and Ismagilov, 2006). We used this approach to encapsulate several thousand cells into single microcompartments.

First, we assessed holding cartridges made of different materials for their suitability to host living cells. For this purpose, we generated 660 nl plugs hosting 3300 Jurkat cells each. While gas-permeable PTFE tubing allowed for cell survival for several days, the use of glass capillaries and vinyl tubing (all with an inner diameter of ∼0.5 mm) resulted in cell death within 24 hr (data not shown). Live/dead stains revealed that, when using PTFE tubing, the survival rate of Jurkat cells remained at ∼90% for the first 2 d, before decreasing gradually from 69% after 3 d, to 38% after 5 d, and finally to 6% after 14 d (Figure 4A). The total number of recovered cells increased from 69% after 1 hr to 194% after 5 d, indicating roughly 1–2 cell divisions (Figure 4C). When repeating the experiments with adherent HEK293T cells, slightly different results were obtained (Figures 4B and 4C). Here, the fraction of viable cells remained above 80% for the first 4 d, before slowly decreasing to 31% after 14 d. The recovery rate increased during the first 5 d from 83% to ∼147%. Recultivation experiments demonstrated the recovery of fully viable and normally proliferating HEK293T cells after 2 d of encapsulation (Figure 4E).

To assess the influence of the cell density on cell survival, we also performed experiments with five and ten times more Jurkat cells per plug. Once again, we obtained an inverse correlation between cell density and survival. Whereas ∼69% viable Jurkat cells were recovered after 3 d when using the initial cell density, only 52% and less than 1% survived when encapsulating five and ten times more cells per plug, respectively (Figure 4D). This massive decrease in cell survival is probably due to the fact that higher cell densities directly resulted in more cells per plug (even at the lowest density, all plugs were occupied), whereas, when encapsulating single cells into drops, the proportion of occupied drops was increased first (with a single cell in a drop still experiencing the same cell density).

In addition, we analyzed if the plugs were subjected to any evaporation during the incubation period. For this purpose, we determined the mean length of the plugs over time by measuring the size of 30 plugs for each time point by using a digital slide gauge and multiplying the mean value by the inner tube diameter to obtain the corresponding plug volumes. No significant decrease in size was observable (Figure 4F), most likely due to the fact that we performed the incubation step in a water-saturated atmosphere (at 37°C, 5% CO_2).

We also investigated the possibility of encapsulating multicellular organisms. Starting with eggs of the nematode *C. elegans*, we analyzed the plugs under the microscope at different time points (Figure 5). Whereas after 2 d hatched worms had already reached the L2–L3 larvae stage, 4 d of encapsulation resulted in the growth of adult worms and the birth of the next generation

(L1 larvae). Longer encapsulation resulted in plugs hosting up to 20 (Movie S2) worms, which finally died after 6–9 d. The passing of individual worms into adjacent microcompartments was never observed, even at high flow rates (up to 1000 µl/hr).

On-Chip Postincubation Analysis of Individual Compartments

High-throughput, cell-based assays require the readout of individual samples after the incubation step (e.g., to screen the phenotype of individual cells within a heterogeneous population). For this purpose, microcompartments stored in a piece of tubing or a reservoir have to be reinjected into an on-chip readout module after the incubation period. To prove the feasibility of this approach, we encapsulated HEK293T cells within 660 pl drops, collected the resulting emulsions, and incubated the samples for 2 and 14 d. Subsequently, the emulsions were reinjected into a chip (same design as for the encapsulation step) and were analyzed microscopically. During reinjection of the emulsion after 2 d of incubation, hardly any coalescence of individual samples was detectable (Figure 6A; Movie S3). After 14 d of incubation, some degree of coalescence was observable; however, the majority of drops (>90%) remained intact. Microscopical comparison of the drops at the time of incubation and reinjection revealed no obvious reduction of the drop size (Figure 6B). This indicates that the drops are not subjected to significant evaporation during the incubation period (within a water-saturated atmosphere).

To demonstrate that the drops can be analyzed individually after reinjection, we encapsulated a population of HEK293T cells that, 2 wk before the experiment, had been incubated in bulk with viral particles (murine leukemia virus pseudotyped with the G protein of the vesicular stomatitis virus) having packaged the *lacZ* gene. The fraction of cells stably expressing the corresponding gene product (β-galactosidase) was ∼13.9%, as determined in an X-Gal assay (Stitz et al., 2001). During the drop production, a fluorogenic substrate (1.7 mM fluorescein di-β-D-galactopyranoside, FDG) for β-galactosidase was coencapsulated into the drops, and a laser beam (488 nm wavelength) was focused onto the channel (downstream of the nozzle). The emitted light was collected in a photomultiplier (Figure 6D) to record the fluorescence signal at t_0. This measurement was performed with the initial population of transduced HEK293T cells and a sample that had been diluted 1:9 with nontransduced HEK293T cells. At the time of encapsulation, no difference in the fluorescence signals was observable, and even drops without any cell showed the same signal intensity (data not shown). After an incubation time of 16 hr at 37°C, the emulsions were reinjected into the chip together with additional fluorinated oil (separately injected into the oil inlet to space out the drops) to repeat the fluorescence measurement (at t_i; analyzing 500 drops/s). Plotting the maximum fluorescence intensity of the drops against the peak width (which corresponds to the drop size and therefore is a good indicator of coalescence) revealed different distinct populations (Figure 6F). Analysis of the peak width proved that even though populations with 2-fold and 3-fold higher volumes were observable, the majority of drops did not coalesce (>93%). In terms of the fluorescence, two main populations with an ∼35-fold difference in their intensity were obtained, as also confirmed by fluorescence microscopy
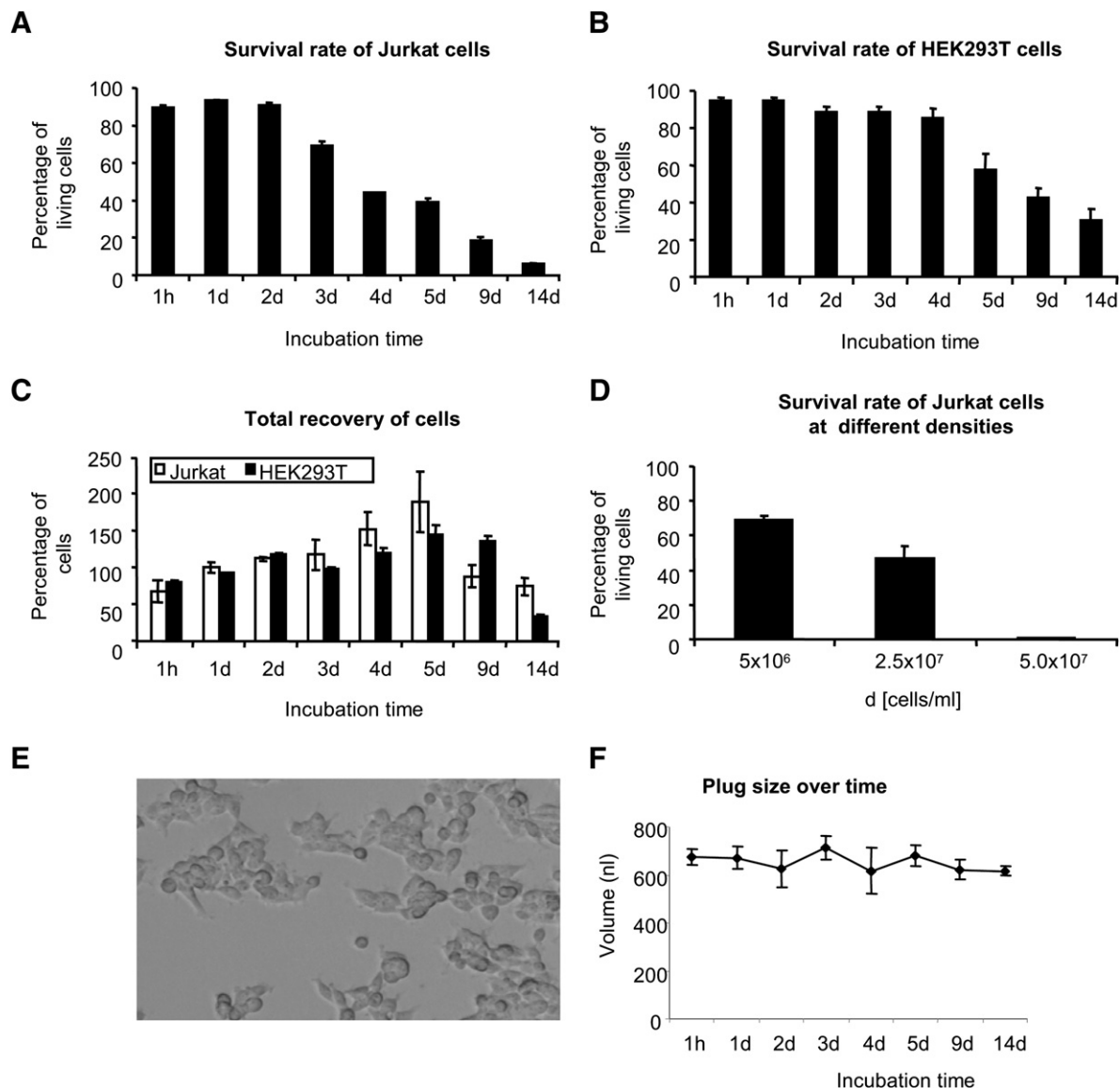
Figure 4. Cell Viability, Recovery, and Recultivation of Cells Encapsulated in 660 nl Plugs

(A and B) The percentage of viable (A) Jurkat and (B) HEK293T cells recovered from plugs at the indicated time points.

(C) The total number of recovered Jurkat and HEK293T cells (live and dead) relative to the number of initially encapsulated cells.

(D) The percentage of viable Jurkat cells encapsulated at different densities after 3 d.

(E) Recultivation of HEK293T cells recovered after 48 hr of encapsulation.

(F) Mean size of plugs harboring HEK293T cells plotted against the incubation time.

Error bars show the standard deviation of three independent experiments.

in which the drops appeared to be either highly fluorescent or nonfluorescent (Figure 6C). Based on these observations, we set gates for the quantitative interpretation of the data (as routinely done in FACS analysis). Gates were set to solely analyze those drops that had not coalesced (corresponding to the populations with the lowest peak width). Based on the way the peak width was defined, fluorescence-positive drops appeared to be bigger (see Figure 6E). Nonetheless, plotting the fluorescence against the peak width enabled noncoalesced drops to be clearly distinguished from coalesced drops for both species (positives and negatives). The use of gating leads to the conclu-

sion that ~5.08% of all noncoalesced drops were fluorescence positive in the sample with nondiluted transduced cells. This number corresponds to ~12.7% of the corresponding cell population when taking into account that only 40.0% of the drops were occupied (as determined by microscopical analysis of the drops during the encapsulation step). This value is in the same range as the fraction of positive cells determined in bulk (~13.9%), by using a conventional X-Gal assay. For the diluted sample, we obtained 0.63% positive drops, corresponding to 1.8% of the cells (34.8% of the drops were occupied). Compared to the nondiluted sample, the negative population showed
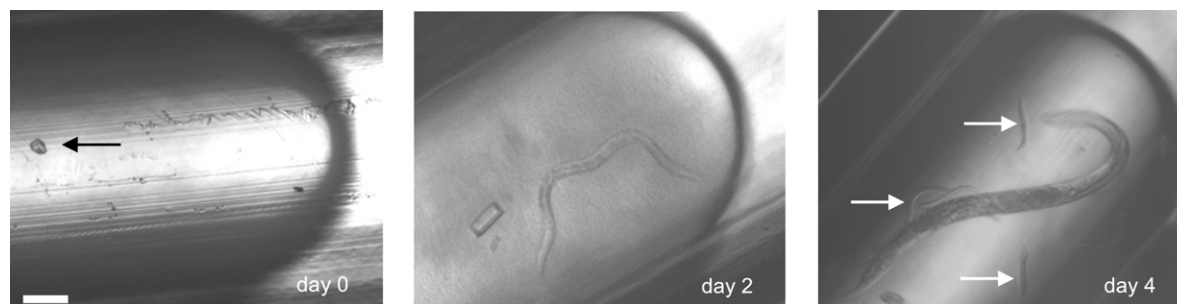
Figure 5. Growth of the Nematode *C. elegans* within Aqueous 660 nl Plugs
Eggs (black arrow) were encapsulated at room temperature, and bright-field microscopical images were taken after 0, 2, or 4 d. White arrows show larvae of the second generation of encapsulated worms. White bar, 100 μm.

a lower fluorescence intensity. This is most likely due to the fact that all drops (even the ones without cells) contain traces of soluble β-galactosidase, resulting from the few dead cells within the syringe (during the encapsulation step). Since the diluted sample contains less enzyme in total, a lower background can be expected, too. Another possible explanation would be the exchange of fluorescein between the drops. However, this seems to be unlikely, since for incubation periods of up to 24 hr we never observed any significant exchange of fluorescein for any surfactants tested (including the ammonium salt of carboxy-PFPE and PEG-PFPE; data not shown). The resulting 7.1-fold difference in terms of positive cells between the samples is in good agreement with the initial 1:9 dilution (assuming an accuracy of ±10% when counting the cultures in a Neubauer chamber before mixing leads to the conclusion that the effective ratio might have been as low as 1:7.4). In summary, these results clearly demonstrate the possibility of quantitatively analyzing individual drops in a high-throughput fashion (we analyzed the drops at a frequency of 500 Hz).

DISCUSSION

We have used droplet-based microfluidic systems to create miniaturized reaction vessels in which both adherent and nonadherent cells can survive for several days. Even though we generated microcompartments with volumes of 660 pl and 660 nl only, in principal almost any volume can be generated by changing the channel sizes and flow rates, or by splitting relatively large microcompartments through a T-junction into smaller units (Adamson et al., 2006). Thus, microcompartments tailored for the encapsulation of small objects like single cells can be generated as well as compartments big enough to host multicellular organisms like *C. elegans*. Furthermore, the size can be adjusted according to the assay duration. Cell density was found to inversely correlate with the survival time of encapsulated cells. Larger compartments are hence preferential for long-term assays, especially since encapsulated cells proliferate within the microcompartments. Consequently, even proliferation assays (e.g., for screening cytostatic drugs) should be possible as long as the chosen volume is big enough to guarantee sufficient supply of nutrition. On the other hand, small volumes might be advantageous for other applications, for example to minimize reagent costs or to rapidly obtain high concentrations of secreted cellular factors. Besides the volume, additional factors, notably the biocompati-

bility of the surfactants and the gas permeability of the storage system, have a major impact on cell survival. Both of the nonionic surfactants described here allowed for cell survival and proliferation, whereas the two ionic surfactants mediated cell lysis. Even though there is no direct proof of correlation, it seemed quite striking that poly-L-lysine, a compound widely used to improve cell attachment to surfaces (Budd et al., 1989), mediated membrane disruption when used as a head group of an ionic surfactant. Long-term incubation also requires sufficient gas exchange. This can be ensured either by using open reservoirs or channels or tubing made of gas-permeable materials such as fluorinated polymers. Efficient gas exchange is also helped by the fact that perfluorocarbon carrier fluids can dissolve more than 20 times the amount of O_2, and 3 times the amount of CO_2, than water and have been shown to facilitate respiratory gas delivery to both prokaryotic and eukaryotic cells in culture (Lowe et al., 1998).

The possibility of reinjecting microcompartments into a chip after the incubation step opens the way for integrated droplet-based microfluidic systems for cell-based HTS. As we have shown here, a fluorescence-based readout of the expression of a cellular reporter gene can be performed in individual compartments at frequencies of 500 Hz. Hence, a wide range of commercially available fluorescence-based assays (Gonzalez and Negulescu, 1998; Sundberg, 2000) can potentially be performed in a high-throughput fashion. The fact that possible coalescence of individual drops does not necessarily bias the readout is noteworthy. As shown here, coalesced drops with higher volumes can easily be identified and excluded from the data analysis. In theory, the use of gates also allows for the analysis of only those compartments hosting a specific number of (fluorescent) cells. In contrast to conventional FACS analysis, the assay readout does not have to be based on fluorophores that remain in, or on the surface of, the cells (e.g., GFP or fluorescent antibodies). Using compartmentalization, we have been able to measure the activity of an intracellular reporter enzyme (β-galactosidase) by using a fluorescent product that is highly membrane permeable (fluorescein).

The integration of additional microfluidic modules into the microfluidic platforms shown here should allow the application range to be expanded. Integrating a microfluidic sorting module (based on dielectrophoresis or valves) (Ahn et al., 2006; Fu et al., 2002) could, for example, enable the screening of drug candidates. In the simplest case, the candidates could be genetically
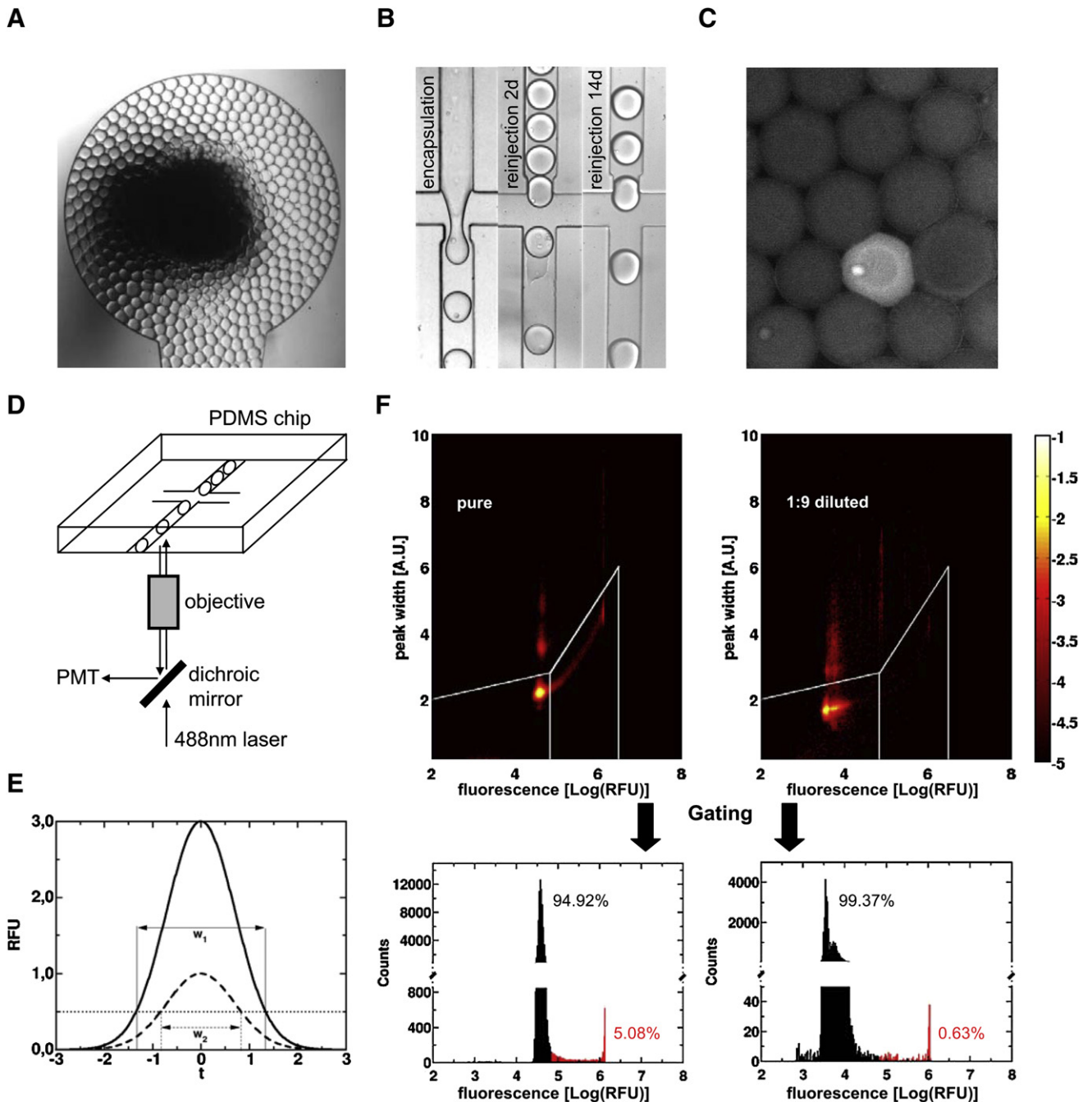
Figure 6. Reinjection and Analysis of Emulsions after Incubation

(A) Bright-field image of the inlet during reinjection of an emulsion (drops containing HEK293T cells) after 2 d of incubation.

(B) Bright-field images of individual drops during encapsulation and after reinjection (off-chip incubation for 2 and 14 d).

(C) Fluorescence-microscopic image of drops hosting *lacZ*-expressing HEK293T cells (converting the fluorogenic substrate FDG) after 16 hr of incubation.

(D) Optical setup for fluorescence measurements.

(E) Influence of the fluorescence intensity (y axis) on the peak width (w). The peak width is defined as the time (t, x axis) for which a fluorescent signal above a certain threshold (dotted, horizontal line) can be measured (due to a drop passing the laser beam). Different fluorescence intensities of the drops (continuous and dashed peaks) result in different apparent peak widths (w_1 and w_2).

(F) Fluorescence signals of drops after reinjection. Upper panels: fluorescence intensity (x axis) plotted against the peak width (y axis) for pure (left) and 1:9 diluted (right) transduced cells. The relative frequency of all events is color coded according to the bar on the right (numbers corresponding to the exponent of the frequency). White gates correspond to noncoalesced drops: left gate, drops considered as negatives; right gate, drops considered as positives. Lower panel: fluorescence intensity (x axis) plotted against the drop counts (y axis) of all events within the gates. Positive events are depicted in red, and negative events are depicted in black.

encoded by the encapsulated cells themselves (starting with a cell library); hence, the collection of sorted positive drops would allow for the identification of hits by DNA sequencing. Alternatively, the sorting module could be used to screen synthetic compounds fixed on beads (e.g., one-bead-one-compound libraries) coencapsulated in the drops. After the sorting step, beads that mediated the desired effect could be recovered from the drops for a subsequent decoding step (e.g., by mass spectroscopy). Using optical barcodes encoding the compound identity might even allow the decoding step to be performed in real time (without the need for a sorting module) (Battersby et al., 2002; Pregibon et al., 2007). For example, different fluorescence channels could be used for the assay and label readout. The fact that the optical barcode does not even have to be directly linked to the test compound when using droplet-based microfluidics is noteworthy: the label can simply be mixed with the test compound prior to the encapsulation step.

SIGNIFICANCE

Aqueous microcompartments can be used as miniaturized vessels for chemical and biological reactions (Tawfik and Griffiths, 1998; Kelly et al., 2007; Griffiths and Tawfik, 2006). We show here how this approach can also be utilized for cell-based applications. We demonstrate that human cells, and even a multicellular organism (*C. elegans*), can be compartmentalized and remain fully viable for several days in droplets. The microfluidic platforms described here allow the encapsulation step to occur at rates of more than 800 per sec. As the number of cells per drop follows a Poission distribution, the optional encapsulation of single cells causes the generation of empty drops, thus decreasing the resulting encapsulation rate to ∼300 per sec. We have demonstrated postincubation fluorescence readout of individual compartments at 500 Hz, and additional droplet manipulation procedures (such as fusion, splitting, and sorting) can be performed at similar rates (Link et al., 2004, 2006; Ahn et al., 2006). Consequently, the throughput of a single integrated, droplet-based microfluidic system for cell-based screening could potentially be 500 times higher than conventional robotic microtiter-plate-based HTS technologies that can perform a maximum of ∼100,000 assays per d, or ∼1 s^{-1}. Using compartments as small as 660 pl, the volume of each assay, and hence the cost of reagents for screening, could be reduced by >1000-fold relative to the smallest assay volumes in microtiter plates (1–2 μl). This may allow many high-throughput biochemical screens to be replaced by more physiologically relevant cell-based assays (Chapman, 2004; Johnston and Johnston, 2002), including assays with highly valuable cells, e.g., primary human cells, which are arguably the most physiologically relevant model systems, but which generally cannot be obtained on the scale required for HTS.

EXPERIMENTAL PROCEDURES

Fabrication of Microfluidic Chips

The microfluidic device (Figure 1A) was fabricated by patterning 75 μm deep channels into poly(dimethylsiloxane) (PDMS) by using soft lithography (Squires

and Quake, 2005). The PDMS was activated by incubation for 3 min in an oxygen plasma (Plasma Prep 2, Gala Instrumente) and was bound to a 50 mm × 75 mm glass slide (Fisher Bioblock). Inlets and outlets were made by using 0.75 mm diameter biopsy punches (Harris Uni-Core). The channels were flushed with a commercial surface-coating agent (Aquapel, PPG Industries) and, subsequently, with N_2 prior to use.

Cells

HEK293T cells were grown and encapsulated in DMEM medium (GIBCO-BRL), and Jurkat cells were grown and encapsulated in RPMI medium (GIBCO-BRL). Both media were supplemented with 10% fetal bovine serum (GIBCO-BRL) and 1% penicillin/streptomycin (GIBCO-BRL). Cells were incubated at 37°C under a 5% CO_2 atmosphere saturated with water.

For fluorescence readouts, the *lacZ* gene was introduced into HEK293T cells by retroviral transduction as described elsewhere (Stitz et al., 2001). In brief, by transfecting HEK293T cells, we generated murine leukemia virus-derived particles (pseudotyped with the G protein of the vesicular stomatitis virus) that had packaged a vector encoding *lacZ*. Two days after transfection, the particles were harvested from the cell-culture supernatants and were used for transduction of fresh HEK293T cells during 1 hr of incubation. Subsequently, the cells were cultivated for 2 wk before encapsulating them together with 1.7 mM fluorescein di-β-D-galactopyranoside (FDG, Euromedex) in drops.

Synthesis of Surfactants

Detailed synthesis and characterization of fluorinated surfactants will be published elsewhere by A.E. and C.H. (unpublished data). In brief, surfactants (Figure 2) were synthesized as follows:

Carboxy-PFPE

To obtain the ammonium salt of carboxy-PFPE, Krytox FS(L) 2000 (DuPont) was reacted with NH_4OH as described (Johnston et al., 1996).

DMP-PFPE

Synthesis of the hydrophilic head group dimorpholinophosphate (DMP) was carried out by reaction of PhEtOH (Aldrich), $POCl_3$ (Fluka), and morpholine (Fluka) with $(Et)_3N$ (Sigma-Aldrich) in THF (Fluka) on ice. Subsequently, DMP was coupled to water/cyclohexane/isopropanol-extracted Krytox FS(H) 4000 (DuPont) by Friedels-Craft-Acylation.

PEG-PFPE

Reaction of Krytox FS(H) 4000 (DuPont) with polyethyleneglycol (PEG) 900 (Sigma) resulted in a mixture of PEG molecules coupled to either one or two PFPE molecules.

Poly-L-Lysine-PFPE

Krytox FS(L) 2000 (DuPont) was reacted with poly-L-Lysine (15,000–30,000; Sigma).

Biocompatibility Test for Different Surfactants

A 100 μl suspension of HEK293T cells ($1.5 × 10^6$ cells/ml in fresh media) was seeded on top of a layer of perfluorocarbon oil (FC40, 3M) in the presence (0.5% w/w) and absence of the tested surfactants. After incubation at 37°C for 0 hr, 24 hr, and 48 hr, bright-light images were taken with a Leica DMIRB microscope.

Drop-Based Encapsulation, Cell Recovery, and Live/Dead Staining

Cells were adjusted to a density of $2.5 × 10^6$ cells/ml (determined with a Neubauer counting chamber), stirred at 200 rpm by using an 8 mm magnetic stir-bar (Roth) in a 5 ml polyethylene syringe (Fisher Bioblock) and injected via PTFE tubing (0.56 mm × 1.07 mm internal/external diameter, Fisher Bioblock) into the microfluidic device (Figure 1A) by using a syringe pump (PHD 2000, Harvard Apparatus) at a flow rate of 1000 μl/hr. The cell suspension was diluted on-chip (see below) by diluting it with sterile media (1000 μl/hr if not otherwise stated), and drops were generated by flow focusing (Anna et al., 2003) of the resulting stream with perfluorinated oil (FC40, 3M), containing 0.5% (w/w) DMP-PFPE (4000 μl/hr). The drop volume was calculated by dividing the flow rate by the drop frequency (determined by using a Phantom V4.2 high-speed camera). Experimental variations in the drop frequency (at constant flow rates) were defined as the degree of polydispersity in terms of the volume (corresponding to the third power of the polydispersity in terms of the diameter when considering a perfect sphere). For each sample, 500 μl of the resulting emulsion was collected within a 15 ml centrifuge tube and

incubated at 37°C within a CO$_2$ incubator (5% CO$_2$, saturated with H$_2$O). After incubation, 250 μl of the emulsion was transferred into a new centrifuge tube and broken by the addition of 15% Emulsion Destabilizer A104 (RainDance Technologies; Guilford, CT) and 10 ml live/dead staining solution (LIVE/DEAD Viability/Cytotoxicity Kit for animal cells, Invitrogen Kit L-3224) and subsequent mixing. After incubation for 3 min (to allow sedimentation of the oil phase), the supernatant was transferred into a 25 cm^2 tissue-culture flask and incubated for 1 hr at room temperature.

On-Chip Dilution of Cells

Drops were generated and diluted on-chip by bringing together two channels containing the cell suspension and sterile media, respectively, and varying the relative flow rates while keeping the overall aqueous flow rate constant at 2000 μl/hr by using two syringe pumps. The number of cells per drop was determined by evaluating movies taken with a high-speed camera (Phantom V4.2) mounted on a microscope. For each dilution, 120 drops were analyzed to determine the number of cells per drop. Subsequently, the data were fitted to a Poisson distribution ($p_{[x = k]} = e^{-\lambda} \times \lambda^k/k!$) by using XmGrace (http://plasma-gate.weizmann.ac.il/Grace/).

Reinjection of Emulsions and Fluorescence Readout of Individual Samples

The emulsions were collected in open syringes (without the plunger being inserted) and incubated within a water-saturated atmosphere (37°C, 5% CO$_2$). During the encapsulation step, a laser beam (488 nm wavelength) was focused onto the channel by using an objective with a 40-fold magnification (Figure 6D, downstream of the nozzle) to excite the fluorophor. Emitted light was diverted by a dichroic mirror (488 nm notch filter), filtered (510 nm ± 10 nm), and collected in a photomultiplier to record the first fluorescence measurement (t_0). After the desired incubation time, mineral oil was added to fill the syringe completely before inserting the plunger and reinjecting the emulsion together with 0.5% w/w DMP-PFPE surfactant in FC40 (injected into the oil inlet to space out the drops) into a chip with the same design as for the encapsulation step. To avoid fragmentation of the drops before the second fluorescence measurement (at t_i), the flow direction was reversed compared to the encapsulation step (the emulsion was injected into the outlet [Figure 1A] to avoid branching channels). All signals from the photomultiplier were recorded by using Labview (National Instruments) and by running an in-house program for the data analysis.

Plug-Based Encapsulation, Cell Recovery, and Live/Dead Staining

To prepare the plugs, 5 × 10^6 cells/ml (determined with a Neubauer counting chamber) were stirred at 510 rpm within a 1.8 ml cryotube (Nunc) by using an 8 mm magnetic stir-bar (Roth) and were kept at 4°C. Subsequently, 660 nl plugs of this cell suspension and perfluorinated oil (FC40, 3M) were aspirated (at 500 μl/hr) into PTFE tubing (0.56 μm × 1.07 mm internal/external diameter, Fisher Bioblock) in an alternating fashion by using a syringe pump (PHD 2000, Harvard Apparatus). For each sample, 30 plugs were loaded before the tubing was sealed (by clamping microtubes to both ends) and were incubated at 37°C within a CO$_2$ incubator (5% CO$_2$, saturated with H$_2$O). After incubation, the plugs were infused into a 25 cm^2 tissue-culture flask. Subsequently, 4 ml live/dead staining solution (LIVE/DEAD Viability/Cytotoxicity Kit for animal cells, Invitrogen Kit L-3224) was added, and the samples were incubated for 1 hr at room temperature. When using adherent cells, the staining solution was additionally supplemented with 0.25 g/l trypsin (GIBCO-BRL) to break up cell clumps.

Determination of the Survival Rates and Total Recovery

After staining, live and dead cells were counted manually by using a microscope (Leica DMIRB) with a UV-lightsource (LEJ ebq 100). For each sample within a 25 cm^2 tissue-culture flask, 30 fields of view (corresponding to ∼4.2 mm^2) were evaluated to calculate the total number of living (green stain) and dead (red stain) cells.

Encapsulation of *C. elegans*

Eggs were resuspended in M9 minimal media (Sigma) supplemented with *E. coli* OP50 (10% w/v of pelleted bacteria). Plugs of the resulting suspension were aspirated into PTFE tubing and incubated at room temperature.

Recultivation Experiments

For recultivation of cells recovered from drops or plugs, semiconditioned medium supplemented with 30% fetal bovine serum (GIBCO-BRL) was added to the cells instead of the staining solution. Cells were then incubated for 2 d at 37°C within a CO$_2$ incubator (5% CO$_2$, saturated with H$_2$O) before imaging with bright-field microscopy.

SUPPLEMENTAL DATA

Supplemental Data include movies of cell encapsulation, the incubation of *C. elegans* in aqueous plugs, and the reinjection of an emulsion and are available at http://www.chembiol.com/cgi/content/full/15/5/427/DC1/.

REFERENCES

Adamson, D.N., Mustafi, D., Zhang, J.X.J., Zheng, B., and Ismagilov, R.F. (2006). Production of arrays of chemically distinct nanolitre plugs via repeated splitting in microfluidic devices. Lab Chip *6*, 1178–1186.

Ahn, K., Kerbage, C., Hunt, T.P., Westervelt, R.M., Link, D.R., and Weitz, D.A. (2006). Dielectrophoretic manipulation of drops for high-speed microfluidic sorting devices. Appl. Phys. Lett. *88*, 24104.

Anna, S.L., Bontoux, N., and Stone, H.A. (2003). Formation of dispersions using "flow focusing" in microchannels. Appl. Phys. Lett. *82*, 364–366.

Battersby, B.J., Lawrie, G.A., Johnston, A.P.R., and Trau, M. (2002). Optical barcoding of colloidal suspensions: applications in genomics, proteomics and drug discovery. Chem. Commun. (Camb.) *14*, 1435–1441.

Beer, N.R., Hindson, B., Wheeler, E., Hall, S., Rose, K., Kennedy, I., and Colston, B. (2007). On-chip, real-time, single-copy polymerase chain reaction in picoliter droplets. Anal. Chem. *79*, 8471–8475.

Budd, J.S., Bell, P.R., and James, R.F. (1989). Attachment of indium-111 labelled endothelial cells to pretreated polytetrafluoroethylene vascular grafts. Br. J. Surg. *76*, 1259–1261.

Chapman, T. (2004). Drug discovery: the leading edge. Nature *430*, 109–115.

Chen, D.L., and Ismagilov, R.F. (2006). Microfluidic cartridges preloaded with nanoliter plugs of reagents: an alternative to 96-well plates for screening. Curr. Opin. Chem. Biol. *10*, 226–231.

Dove, A. (1999). Drug screening–beyond the bottleneck. Nat. Biotechnol. *17*, 859–863.

Fu, A.Y., Chou, H.-P., Spence, C., Arnold, F.H., and Quake, S.R. (2002). An integrated microfabricated cell sorter. Anal. Chem. *74*, 2451–2457.

Funfak, A., Brösing, A., Brand, M., and Köhler, J.M. (2007). Micro fluid segment technique for screening and development studies on *Danio rerio* embryos. Lab Chip *7*, 1132–1138.

Gonzalez, J.E., and Negulescu, P.A. (1998). Intracellular detection assays for high-throughput screening. Curr. Opin. Biotechnol. *9*, 624–631.

Griffiths, A.D., and Tawfik, D.S. (2006). Miniaturising the laboratory in emulsion droplets. Trends Biotechnol. *24*, 395–402.

Grodrian, A., Metze, J., Henkel, T., Martin, K., Roth, M., and Köhler, J.M. (2004). Segmented flow generation by chip reactors for highly parallelized cell cultivation. Biosens. Bioelectron. *19*, 1421–1428.

Hawtin, P., Hardern, I., Wittig, R., Mollenhauer, J., Poustka, A., Salowsky, R., Wulff, T., Rizzo, C., and Wilson, B. (2005). Utility of lab-on-a-chip technology for high-throughput nucleic acid and protein analysis. Electrophoresis *26*, 3674–3681.

He, M., Edgar, J.S., Jeffries, G.D.M., Lorenz, R.M., Shelby, J.P., and Chiu, D.T. (2005). Selective encapsulation of single cells and subcellular organelles into picoliter- and femtoliter-volume droplets. Anal. Chem. *77*, 1539–1544.

Huebner, A., Srisa-Art, M., Holt, D., Abell, C., Hollfelder, F., deMello, A.J., and Edel, J.B. (2007). Quantitative detection of protein expression in single cells using droplet microfluidics. Chem. Commun. (Camb.) *Mar 28*, 1218–1220.

Johnston, K.P., Harrison, K.L., Clarke, M.J., Howdle, S.M., Heitz, M.P., Bright, F.V., Carlier, C., and Randolph, T.W. (1996). Water-in-carbon dioxide microemulsions: an environment for hydrophiles including proteins. Science *271*, 624–626.

Johnston, P.A., and Johnston, P.A. (2002). Cellular platforms for hts: three case studies. Drug Discov. Today *7*, 353–363.

Kelly, B.T., Baret, J.-C., Taly, V., and Griffiths, A.D. (2007). Miniaturizing chemistry and biology in microdroplets. Chem. Commun. (Camb.) *May 14*, 1773–1788.

Li, P.C., and Harrison, D.J. (1997). Transport, manipulation, and reaction of biological cells on-chip using electrokinetic effects. Anal. Chem. *69*, 1564–1568.

Lin, Y.H., Lee, G.B., Li, C.W., Huang, G.R., and Chen, S.H. (2001). Flow-through sampling for electrophoresis-based microfluidic chips using hydrodynamic pumping. J. Chromatogr. A. *937*, 115–125.

Link, D.R., Anna, S.L., Weitz, D.A., and Stone, H.A. (2004). Geometrically mediated breakup of drops in microfluidic devices. Phys. Rev. Lett. *92*, 054503.

Link, D.R., Grasland-Mongrain, E., Duri, A., Sarrazin, F., Cheng, Z., Cristobal, G., Marquez, M., and Weitz, D.A. (2006). Electric control of droplets in microfluidic devices. Angew. Chem. Int. Ed. Engl. *45*, 2556–2560.

Lowe, K.C., Davey, M.R., and Power, J.B. (1998). Perfluorochemicals: their applications and benefits to cell culture. Trends Biotechnol. *16*, 272–277.

Margulies, M., Egholm, M., Altman, W.E., Attiya, S., Bader, J.S., Bemben, L.A., Berka, J., Braverman, M.S., Chen, Y.J., Chen, Z., Dewell, S.B., et al. (2005). Genome sequencing in microfabricated high-density picolitre reactors. Nature *437*, 376–380.

Martin, K., Henkel, T., Baier, V., Grodrian, A., Schön, T., Roth, M., Köhler, J.M., and Metze, J. (2003). Generation of larger numbers of separated microbial populations by cultivation in segmented-flow microdevices. Lab Chip *3*, 202–207.

Oh, H.J., Kim, S.H., Baek, J.Y., Seong, G.H., and Lee, S.H. (2006). Hydrodynamic micro-encapsulation of aqueous fluids and cells via 'on the fly' photo-polymerization. J. Micromech. Microeng. *16*, 285–291.

Pregibon, D.C., Toner, M., and Doyle, P.S. (2007). Multifunctional encoded particles for high-throughput biomolecule analysis. Science *315*, 1393–1396.

Sakai, S., Kawabata, K., Ono, T., Ijima, H., and Kawakami, K. (2005). Higher viscous solution induces smaller droplets for cell-enclosing capsules in a co-flowing stream. Biotechnol. Prog. *21*, 994–997.

Shendure, J., Porreca, G.J., Reppas, N.B., Lin, X., McCutcheon, J.P., Rosenbaum, A.M., Wang, M.D., Zhang, K., Mitra, R.D., and Church, G.M. (2005). Accurate multiplex polony sequencing of an evolved bacterial genome. Science *309*, 1728–1732.

Song, H., Tice, J.D., and Ismagilov, R.F. (2003). A microfluidic system for controlling reaction networks in time. Angew. Chem. Int. Ed. Engl. *42*, 768–772.

Song, H., Li, H.-W., Munson, M.S., Ha, T.G.V., and Ismagilov, R.F. (2006). On-chip titration of an anticoagulant argatroban and determination of the clotting time within whole blood or plasma using a plug-based microfluidic system. Anal. Chem. *78*, 4839–4849.

Squires, T.M., and Quake, S.R. (2005). Microfluidics: fluid physics at the nanoliter scale. Rev. Mod. Phys. *77*, 977–1026.

Srinivasan, V., Pamula, V.K., and Fair, R.B. (2004). An integrated digital microfluidic lab-on-a-chip for clinical diagnostics on human physiological fluids. Lab Chip *4*, 310–315.

Stitz, J., Mühlebach, M.D., Blömer, U., Scherr, M., Selbert, M., Wehner, P., Steidl, S., Schmitt, I., König, R., Schweizer, M., et al. (2001). A novel lentivirus vector derived from apathogenic simian immunodeficiency virus. Virology *291*, 191–197.

Sundberg, S.A. (2000). High-throughput and ultra-high-throughput screening: solution- and cell-based approaches. Curr. Opin. Biotechnol. *11*, 47–53.

Tawfik, D.S., and Griffiths, A.D. (1998). Man-made cell-like compartments for molecular evolution. Nat. Biotechnol. *16*, 652–656.

Thorsen, T., Roberts, R.W., Arnold, F.H., and Quake, S.R. (2001). Dynamic pattern formation in a vesicle-generating microfluidic device. Phys. Rev. Lett. *86*, 4163–4166.

Thorsen, T., Maerkl, S.J., and Quake, S.R. (2002). Microfluidic large-scale integration. Science *298*, 580–584.

Umbanhowar, P.B., Prasad, V., and Weitz, D.A. (2000). Monodisperse emulsion generation via drop break off in a coflowing stream. Langmuir *16*, 347–351.

Villarino, A., Bouvet, O.M., Regnault, B., Martin-Delautre, S., and Grimont, P.A.D. (2000). Exploring the frontier between life and death in *Escherichia coli*: evaluation of different viability markers in live and heat- or uv-killed cells. Res. Microbiol. *151*, 755–768.

Wang, J. (2002). On-chip enzymatic assays. Electrophoresis *23*, 713–718.

Wheeler, A.R., Moon, H., Bird, C.A., Loo, R.R.O., Kim, C.-J.C.J., Loo, J.A., and Garrell, R.L. (2005). Digital microfluidics with in-line sample purification for proteomics analyses with maldi-ms. Anal. Chem. *77*, 534–540.